

Crystallization of Syndiotactic Polystyrene in β -Form. 4. Crystal Structure of Melt-Grown Modification

Masatoshi Tosaka,* Masaki Tsuji, Shinzo Kohjiya, Laurent Cartier,[†] and Bernard Lotz[†]

Division of States and Structures, Institute for Chemical Research, Kyoto University, Uji, Kyoto-fu 611-0011, Japan

Received July 6, 1998; Revised Manuscript Received March 16, 1999

ABSTRACT: The propriety of the theory presented in the authors' previous paper [Tosaka et al. *Macromolecules* 1997, 30, 6592], which predicted that monoclinic crystallites are the majority in the β' -modification of syndiotactic polystyrene, was assessed by examining the structure of the modification. The electron diffraction patterns from the single-crystal-like lamellae of β' -modification showed a streaked feature which supports our prediction. The high-resolution images evidenced that the β' -modification is composed of monoclinic domains; the boundary between the domains is a twin plane. This feature was also detected in the dark-field images as irregularly spaced striations. The probability, p , to find the same type of bimolecular layer (viz., a motif) at the next position of a motif was estimated from the high-resolution and the dark-field images. The subsequent energetic analysis based on the experimental p values showed that the theory presented in the previous paper is reasonable.

Introduction

The syndiotactic polystyrene (s-PS) β -form^{1–6} is distinguished by a trans-planar conformation of the backbone chains and the orthorhombic unit cell ($P2_12_12_1$, $a = 2.87$ nm, $b = 0.88$ nm, c (chain axis) = 0.51 nm; our assignment of a - and b -axes is different from other researchers).^{1,2,7,8} A characteristic of the β -form is the existence of a kind of structural disorder, which we designate stacking faults.^{2–4} The crystal structure of the β -form without the fault is regarded as a regular alternation of two types of bimolecular layers, viz., motifs. This regular structure is to be orthorhombic with $P2_12_12_1$ symmetry. On the other hand, the stacking fault is a succession of the motifs of a same type. The faulted part is related to a monoclinic cell with half the volume of the orthorhombic (regular) one. That is, the β -form with stacking faults results from the coexistence of monoclinic layers in the orthorhombic crystal.

Another characteristic of the β -form is the existence of two crystalline modifications. Guerra et al.¹ have found that the β -form shows two types of extinction rules in the X-ray diffractogram according to the preparation conditions. Intensity peaks corresponding to the orthorhombic $hk0$ reflections with $h + k = \text{odd}$ do not exist in the diffractogram of the melt-crystallized specimen. This crystalline form was named the β' -modification. The other form in which $hk0$ reflections with $h + k = \text{odd}$ exist was named the β'' -modification. While the β' -modification was found mostly in the melt-crystallized specimen, the β'' -modification was found in the specimens prepared by isothermal crystallization from a dilute solution,^{2–4} by annealing the δ -form,⁷ or by casting from solution.¹

The structural difference between the β' - and β'' -modifications was explained by De Rosa et al.⁸ in terms

of the stacking fault as follows: A statistical occurrence of the stacking fault produces a pseudocentering in the ab -projection of the crystal lattice, resulting in the space group $Cmcm$ (in which $hk0$ reflections with the odd numbers of $h + k$ are extinct). The β' -modification may be very close to this limiting disordered structure, while the limiting ordered β'' -modification corresponds to a regular alternation of motifs of A and B (space group $P2_12_12_1$).

In this paper, the specimen of the β' -modification was prepared above the "critical temperature"⁵ (ca. 220 °C) from the melt, and the structure was investigated by transmission electron microscopy in order to verify the validity of our view (which will be presented shortly) and to confirm the extensibility of the previous analysis (for solution crystallization)⁵ to the case for melt crystallization.

Theoretical Treatment

Here, we present briefly our theory.⁵ At first, we obtained the "probability of presence of the stacking faults", p , experimentally for solution grown single crystals of the β -form.⁴ (This probability value, p , was defined in the first paper² of this series as the probability that we find the same type of motif at the next position of a given motif in a crystal. This definition of p is consistent throughout all our works,^{3–5} though we have expressed p as the "probability of presence of the stacking faults" for convenience.) Then we assumed a model of the incorporation mechanism⁵ of the stacking faults into a crystal, to explain the dependence of p on the crystallization temperature (T_c). In the model, the p value is determined as a result of growth competition between two types of crystalline layers, i.e., the orthorhombic ("regular") and the monoclinic ("faulted") ones; the growth rate in the stacking direction for the alternation of two types of motifs ($-AB-$ or $-BA-$) comprising the orthorhombic ("regular") layer is G_R , and the rate for the succession of motifs of same type ($-AA-$ or $-BB-$) comprising the monoclinic ("faulted") layer is G_F . On the basis of the growth theory of polymer

[†] Institut Charles Sadron, 6 Rue Boussingault, 67083 Strasbourg, France.

* To whom all correspondence should be addressed. Tel +81-774-38-3063; Fax +81-774-38-3069; e-mail tosaka@scl.kyoto-u.ac.jp.

crystals proposed by Hoffman and co-workers,^{9,10} each growth rate was formulated as follows:

$$G_R = C \exp[-KT_d^0/T_c(\Delta T)(\Delta h_f)f]$$

$$G_F = C \exp[-KT_d^0/T_c(\Delta T_F)(\Delta h_f - \Delta E)f_F] \quad (1)$$

where C is the parameter containing several factors, for example the activation energy of diffusion in solution and so on; K is a constant;⁵ T_d^0 and ΔT are the equilibrium dissolution temperature and the supercooling, respectively (the subscript, F , indicates the faulted structure); and Δh_f and $\Delta h_f - \Delta E$ are the heat of fusion for the orthorhombic layer and that for the monoclinic layer, respectively. The factors f and f_F were introduced to correct the heat of fusion at high undercooling and are given by⁹

$$f = 2T_c/(T_d^0 + T_c)$$

$$f_F = 2T_c/(T_d^0 + T_c) \quad (2)$$

These factors were canceled out in the final formulation of p , and accordingly, they disappeared in our previous paper.⁵ In short, the growth rates, G_R and G_F , were assumed to be different because of the difference, ΔE , in the heat of fusion. The positive value of ΔE means that the alternation of two types of motifs (viz., the orthorhombic layer) is more stable than the succession of same motifs and is the majority in the crystal, resulting in $p < 0.5$.

Assuming that $p = G_F/(G_R + G_F)$, the T_c dependence of p was formulated as follows:

$$p = 1/[1 + \exp\{K(T_d^0)^2\xi/T_c(\Delta h_f)(\Delta T)(\Delta T - \xi T_d^0)\}] \quad (3)$$

where $\xi = \Delta E/\Delta h_f$.

The attempt to fit the theoretical expression of p (viz., eq 3) to the experimental T_c dependence has led us to the following view:

(1) If ΔE has a certain positive value which is independent of T_c , the p value should decrease abruptly as T_c approaches T_d^0 , as is shown in Figure 3 of ref 5. Since the treatment is purely theoretical, this tendency should be general for the formation of this kind of faults caused by the coexistence of two types of structures.

(2) Since the T_c dependence of p is not successfully explained if the constant ΔE is assumed, we judged that ΔE should vary with T_c . By rearranging eq 3, we obtained the following formulation:

$$\xi = T_c(\Delta T)^2 \ln[(1-p)/p]/\{(K/\Delta h_f)(T_d^0)^2 + T_c(\Delta T)(T_d^0) \ln[(1-p)/p]\} \quad (4)$$

Then, by putting the experimental p values into this equation, the T_c dependence of ξ ($=\Delta E/\Delta h_f$) was evaluated. The result has led to an important conclusion that the relative energy difference, ξ , between the orthorhombic and the monoclinic crystallites of the β -form decreases linearly with increasing T_c , at least on the growing surface of the crystal. (It should be noted that the variation of ξ directly means the variation of ΔE because Δh_f is constant regardless of temperature. The factors f and f_F in eqs 1 and 2 express the temperature dependence of Δh_f ; see section 2.4 of ref 9.) On the basis of the T_c dependence of ξ , ΔE is expected to become

negative when T_c is above a certain critical temperature (ca. 220 °C). The negative value of ΔE means that the succession of motifs of same type (viz., the monoclinic layer) is more stable than the alternation of two types of motifs and is the majority in a crystal ($p > 0.5$). Such a crystal should be attributed to the β' -modification according to the expected systematic absence of diffraction.^{4,5} (Features of this kind in the ED pattern are explained by the formulation of intensity distribution, viz., eqs 7 and 8, which will be shown later.) In other words, we predicted that a different "order" will take place above the critical temperature so that the β' -modification may not be a "limiting disordered" structure.

All the formulation mentioned above for solution crystallization is, of course, applicable for crystallization from the melt, only by replacing T_d^0 with T_m^0 (the equilibrium melting temperature).

Experimental Section

Sample Preparation. The s-PS ($M_w = 1.6 \times 10^5$) was kindly supplied by Idemitsu Petrochemical Co., Ltd., and was used without further purification. To observe with a transmission electron microscope (TEM), thin specimens of the β' -modification were prepared by the following procedure. The s-PS was dissolved in cyclohexanone at about 150 °C to be a 0.58 wt % solution. Then a thin film of s-PS was formed by putting a drop of the solution onto a surface of water. The thin film was picked up onto a glass slide and dried. The s-PS thin film on the glass slide was melted at 300 °C for 1 min with a heating stage (Mettler FP80). The melt was cooled to a prefixed T_c ranging from 230 to 260 °C at a rate of 20 °C/min, kept at the temperature for 10 min, taken out of the stage, and then cooled to room temperature. On cooling the s-PS from the melt, the growth rate may have a maximum around 223 °C.¹² Accordingly, we expected that nearly isothermal crystallization of the specimens can be achieved by this preparation method, at least around 223 °C. The reason why we did not quench the melt to the prefixed T_c is to avoid the growth of another crystalline form, viz. the α -form.¹

For morphological observation, the s-PS specimen on the glass slide was shadowed with gold at a shadowing angle θ ($= \tan^{-1} 1/4$) and reinforced with vapor-deposited carbon. For dark-field (DF) and high-resolution electron microscopy (HREM) observation, however, only carbon was evaporated. A drop of aqueous solution of poly(acrylic acid) was put on the specimen and dried. The specimen was scraped together with the solidified poly(acrylic acid) out of the glass slide with a razor blade. The poly(acrylic acid) was dissolved away by putting it on the surface of water, leaving the s-PS specimen there. The floating s-PS specimen was picked up onto a copper grid or onto a "Triafol" microgrid mounted on a copper grid for transmission electron microscopy.

Morphological Observation. The specimen was investigated with a TEM (JEOL JEM-200CS) operated at 200 kV. Photographic films (Kodak SO-163 or Mitsubishi MEM) were used for recording the images and ED patterns and developed for 5 min in the full-strength Mitsubishi Gekko developer.

Dark-Field Imaging. The specimen was investigated with a TEM (JEOL JEM-200CS) operated at 160 or 200 kV. For DF imaging, a single diffraction spot could not be separately used due to the large size of the objective aperture, but several diffraction spots (e.g., 110, 310, 510, 220, 420) were used together.³ Both types of photographic films were used and developed as above.

High-Resolution Observation. HREM images were taken with a cryo-TEM (JEOL JEM-400SFX) operated at 400 kV using a built-in minimum dose system (MDS) at a direct magnification of 1×10^5 . In this case, the specimen mounted on a microgrid was cooled to the liquid helium temperature (4.2 K) to suppress radiation damage. The electron dose on the specimen for taking one micrograph was set at an exposure

of 7×10^3 electrons/nm² for Mitsubishi MEM films, which were developed for 10 min in the full-strength Mitsubishi Gekko developer.

Results and Discussion

Before starting discussion on the results obtained newly in this work, following two points should be considered:

(1) Variation of p with T_c : According to the Boltzmann law, the population of the high-energy state ought to increase with increasing T_c . Is it reasonable to assume that the value of p will decrease with increasing T_c , if the energy difference ΔE is constant? Is our idea applicable to other polymer crystals in which similar faulted structures are incorporated (i.e., the case where two types of structures coexist)?

(2) T_c dependence of ξ : There are some assumptions in our treatment. How reliable is the T_c dependence of ξ ?

In this context, the discussion concerns not only the specific polymer crystal, viz., the s-PS β -form, but also the general tendency of the variation of faulted structures according to T_c . Establishment of a route to obtain the less (or the more) faulted polymer crystals may be significant not only from the scientific but also from the industrial viewpoint.

As for the first point mentioned above, the Boltzmann law has already been considered when the growth rates, G_R and G_F , were formulated. According to the growth theory of polymer crystals,^{9,10} the growth rate is determined by both the forward (stem deposition) and the backward (stem removal) reactions. The rate constant of the forward reaction is determined by the activation energy of the stems to the "segmentalized-aligned activated complex",¹⁰ which may not be different for the orthorhombic and the monoclinic crystallites. On the other hand, the rate constant of the backward (stem removal) reaction is determined by the free energy of fusion, ΔG . These rate constants were formulated using the Boltzmann law. The backward reaction of the high-energy ("faulted") structure is much enhanced as T_c approaches T_d^0 (or T_m^0) because ΔG approaches zero faster than that for the low-energy ("regular") structure. Accordingly, the growth rate of the high-energy structure should be relatively lowered with increasing T_c . As a result, p may decrease at higher T_c 's if ΔE is constant. We can find an example that is consistent with our idea in the case of syndiotactic polypropylene (s-PP). Single crystals of s-PP also contain certain faults that are caused by the coexistence of two types of structures and show a streaked feature in the electron diffraction (ED) pattern. With an increase in T_c , the degree of spread of the streaked reflections that are caused by the faults evidently decreases,¹¹ as is deduced from the tendency shown in Figure 3 of ref 5.

Before discussing the second point, at first, the T_c dependence of p ,^{4,5} on which our analysis is based, should be considered. A weak T_c dependence was observed for p , and p seemed roughly constant (Figure 4 of ref 5). Has the T_c dependence of ξ that was derived from a "fixed" p value accidentally shown the linear relationship? We strongly believe that the "weak T_c dependence" of p is essential for the linear T_c dependence of ξ , since we have confirmed that such a fixed p value will never lead to the linearity shown in Figure 4 of ref 5. However, the linearity itself does not warrant our theory. One of the way to ensure the propriety of a

theory is to predict a phenomenon and to prove it experimentally. The prediction derived from our theory is that the monoclinic crystallites are the majority ($p > 0.5$) in a crystal grown above the critical temperature.⁵ This is neither the "limiting disordered" structure proposed by De Rosa et al.⁸ nor the simple consequence, $p = 0.5$, derived below by using the Boltzmann law.

The population of the states is determined on the basis of the Boltzmann law,

$$n_F/n_R = \exp[-(\epsilon_F - \epsilon_R)/kT] \quad (5)$$

If the population of the faulted structure, n_F , is simply determined by this law regardless of the consideration of growth rate, then p may be formulated as follows:

$$p = n_F/(n_R + n_F) = 1/\{1 + \exp[(\epsilon_F - \epsilon_R)/kT]\} \quad (6)$$

In eqs 5 and 6, n , ϵ , k , and T are the population, the energy state, the Boltzmann constant, and the temperature, respectively. Subscripts R and F indicate the low-energy ("regular") and the high-energy ("faulted") structures, respectively. Though this formulation may be somewhat oversimplified, it expresses well the idea that the population of high-energy state will increase with increasing T . According to eq 6, p should approach the maximum value 0.5 with increasing T_c , if $(\epsilon_F - \epsilon_R)$ which is directly related to ΔE defined in Theoretical Treatment is constant. Any modification of this equation will lead to p values smaller than 0.5. The β' -modification, for which the systematic absences in diffraction is explained only when $p \geq 0.5$,⁴ must correspond to the extreme case with $p = 0.5$ if based on this idea. On the other hand, we predicted that $p > 0.5$ above a certain critical T_c .⁵ That is, if the value of p is estimated to be greater than 0.5 in the β' -modification, our theory must be more confident than the idea represented by eq 6, and at the same time, our view for the T_c dependence of fault-population will be supported.

Morphological Observation. We judged, on the basis of morphological observation, whether or not the specimen could be grown isothermally at the desired T_c . Figure 1 shows the morphology of the specimen grown at 240 °C. The corresponding ED pattern (inset of Figure 1) in which the reflections with $h + k = \text{odd}$ are absent (see Figure 2b) shows that the crystal in the specimen is the β' -modification and that the molecular chain stems are aligned parallel to the incident electron beam direction. Each sharp reflection in the ED pattern arced only slightly, and hence, this crystal can be regarded as a single-crystal-like lamella. The outline of the lamella is mostly elongated along the b -axis direction. Thin cracks shown in Figure 1 may have been caused by the shrinkage of the specimen during cooling to room temperature. Judging from the effect of shadowing, the crystalline region is bordered with thinner terraces (indicated with arrowheads in Figure 1). In some of the specimens grown at 250 °C, spherulitic texture was observed instead of the flat terraces. Apparent fluctuation of the lamellar thickness inside the crystal bordered with the terraces (or spherulites) is not found in Figure 1, except the cracks. Because the lamellar thickness of the β -form shows the T_c dependence⁸ in the case of solution crystallization,⁴ and the dependence is also detected in this case as the existence of such thinner terraces, we judged that most of the part inside the crystal surrounded by the terraces may have grown nearly isothermally; only the terraces may be the part

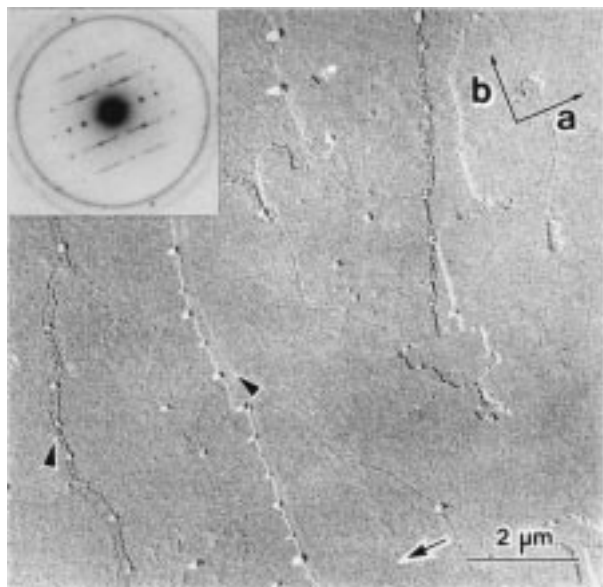


Figure 1. Morphology of the melt-grown lamella of s-PS grown at 240 °C. The arrow shows the shadowing direction. The inset shows the corresponding ED pattern. Outline of a lamella is bordered with thinner terraces which are indicated with arrowheads.

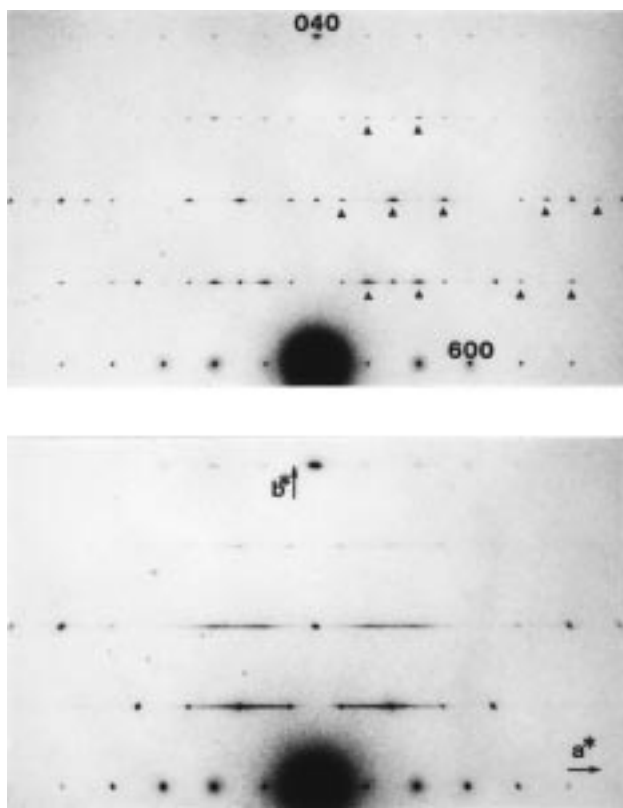


Figure 2. ED patterns of the s-PS β' -form. (a, top) β'' -modification grown from a dilute solution at 200 °C. Arrowheads indicate streaked reflections with $h + k = \text{odd}$. (b, bottom) β' -modification grown from the melt at 240 °C. Reflections with $h + k = \text{odd}$ are absent.

grown in the cooling process. Specimens prepared at T_c 's between 230 and 250 °C showed similar features in their morphologies and in their ED patterns. These specimens were, therefore, also regarded as isothermally crystallized ones. However, in the specimens prepared above 255 °C, almost no large lamellae were found; small

lamellae buried in spherulites were mostly observed. Accordingly, the specimens prepared only from 230 to 250 °C were used for the subsequent quantitative analysis.

Diffraction Intensity. The most prominent and the most confidential information to estimate whether $p = 0.5$ or $p > 0.5$ in the β' -modification was obtained by the analysis of the diffraction intensity distribution, on the basis of following equations:^{2,4}

(a) $V = \text{even}$

$$I \propto \frac{J_1 + J_2}{2} \sum_n \delta(U - 2n) + \frac{J_1 - J_2}{2} \frac{1 - (1 - 2p)^2}{1 - 2(1 - 2p) \cos[\pi(U + 1)] + (1 - 2p)^2} \quad (7)$$

(b) $V = \text{odd}$

$$I \propto \frac{J_1 + J_2}{2} \sum_n \delta(U - 2n - 1) + \frac{J_1 - J_2}{2} \frac{1 - (1 - 2p)^2}{1 - 2(1 - 2p) \cos(\pi U) + (1 - 2p)^2} \quad (8)$$

where I is the intensity and U and V are coordinates in the reciprocal space, which can be replaced by h and k , respectively, having real values. J_1 and J_2 are structure factors defined in ref 2 or 4, and δ is Dirac's δ -function. The first terms in both equations correspond to the sharp spotlike reflections located at reciprocal lattice points (RLPs) with $h + k = \text{even}$.

The second terms in eqs 7 and 8 express the intensity distributions of the streaks. (The schematic representation of the ED pattern based on the formulation of diffraction intensity is shown for $p < 0.5$ and also for $p > 0.5$ in Figure 2 of ref 4.) If $p = 0.5$, the streak must be "continuous" because the second terms become independent of U . The intensity distribution of this continuous streak should represent directly the molecular transform (viz., a combined structure factor, $(J_1 - J_2)/2$). On the other hand, if $p > 0.5$, the intensity profiles of the streaks represent the molecular transform modulated by a function of U so that the intensities at the RLPs with $h + k = \text{odd}$ become minima. Accordingly, the judgment is possible whether or not the observed intensity distribution of the streak is modulated by the function of U , i.e., whether the intensities at RLPs with $h + k = \text{odd}$ are minima.

The ED pattern of the melt-grown lamella (β' -modification, $T_c = 240$ °C) and that of the solution-grown single crystal (β'' -modification)^{2,3} are shown in parts b and a of Figure 2, respectively. It is evident that the features in these ED patterns are perfectly consistent with those expected from eqs 7 and 8. In the case of the β'' -modification (Figure 2a), the streaked reflection has the maximum intensity at each RLP with $h + k = \text{odd}$. On the other hand, in the case of the β' -one (Figure 2b), the maximum of a streak is located at each RLP with $h + k = \text{even}$, and accordingly, 220 and 420 have stronger intensity; the intensities at RLPs with $h + k = \text{odd}$, e.g., at 320, have turned to minima. Furthermore, the intensity relationship among spotlike reflections with $h + k = \text{even}$ seems to be maintained between these ED patterns, judging from the reflections

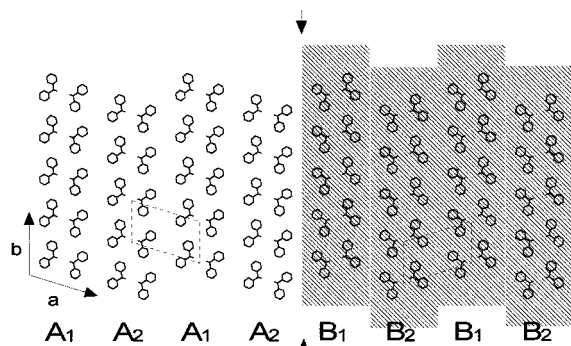


Figure 3. Packing model for the s-PS β' -modification. Arrows indicate the domain boundary. Broken lines indicate the monoclinic unit cell.

that are not overlapped with strong streaks. This observation is also consistent with eqs 7 and 8 in which the components of intensities contributing to spotlike reflections (first terms in eqs 7 and 8) are independent of p . That is to say, the formulation of diffraction intensity, on which the following discussion will be based, should be reliable.

Though the detail is not shown here, we could confirm that the observed streaks are modulated by the function of U , based on the comparison with the calculated structure factor. Such confirmation is also possible simply by comparing, between parts a and b of Figure 2, the intensities at the 320 or 520 RLP. Though the structure factor at 320 is strong enough as is known from the corresponding reflection in Figure 2a, the intensity is very weak in Figure 2b, indicating the intensity distribution of the streak is modulated. Accordingly, the β' -modification which showed the ED pattern in Figure 2b corresponds to the case for $p > 0.5$.

The structure of the β' -modification should be modeled as is shown in Figure 3 for the exact understanding of the HREM and DF images which shall be shown shortly. The consecutive motifs of a same type will comprise a domain elongated in the direction parallel to the b -axis. In each domain, the unit cell can be defined to be monoclinic (plausible space group = $P2_1/m$), if we assume that mutual arrangement of phenyl rings along the c -axis is identical with that proposed in refs 7 and 8. (For convenience, the orthorhombic unit cell will be used for the crystallographic indication in this article.) The boundary between the domains is a twin plane. It should be noted that the arrows in Figure 3 indicate the location of the domain boundary, not of the "stacking fault". (The arrows, however, indicated the "stacking fault" in Figure 1 of our previous paper.⁵) That is to say, the monoclinic crystallite is the second "regular" structure in the β' -modification so that the domain boundary between two monoclinic crystallites, where two types of motifs alternate, is a twin boundary. The molecular arrangement illustrated in Figure 3 was really observed in the HREM image of the melt-grown lamella.

HREM Images. Figure 4 shows the HREM image⁶ of the specimen grown at 245 °C, which was taken at 4.2 K with the cryo-TEM. The inset is the optical diffractogram of the original negative. The streaked feature of the diffractogram shows that the information concerning the arrangement of molecular stems is to be sufficiently recorded in this HREM image. Each dark dot should correspond to the projected molecular stem viewed along its axis. As is illustrated in Figure 3, the

arrangement of the dark dots in Figure 4 shows that the crystal is composed of monoclinic domains.

The lateral width of the domain in the a -axis direction is up to 7 nm in Figure 4, corresponding to the width of five motifs. Even in the HREM images of the specimens grown at different T_c 's, we could also identify similar domains. Such a domain consisting of a long succession of the motifs of one type has never been observed in the HREM images of the β'' -modification.^{2,3}

DF Images. As is easily presumed, the domain structure presented in Figure 3 was also detected in the DF images. Figure 5 shows a DF image of the melt-crystallized specimen, which was taken by using several $hk0$ reflections.³ As was seen in the DF images of the solution-grown single crystals (viz., the β'' -modification),³ many striations are running parallel to the b -axis direction. However, Figure 5 should be interpreted in a different way from that in ref 3, according to the result of ED and HREM experiments. The bright and dark striations should be attributed to the location of a monoclinic domain which is made of, e.g., motifs A only and motifs B only, respectively.²⁻⁴ The lateral width of the bright striations in Figure 5 ranged between 2 and 8 nm, which agree well with those estimated from the HREM images. Between the bright and the dark striations, there should be one alternation of motifs A and B, namely the domain boundary. Accordingly, there should be two domain boundaries on both sides of, for example, one bright striation.

Dependence of the Energetic Difference between "Regular" and "Faulted" Structures on the Crystallization Temperature. Here, the p values were estimated from the DF images and the computer-processed⁶ HREM ones by counting the number of domains in the unit length. Figure 6 is the T_c dependence of p estimated for the melt-grown β' -modification. There is a considerably broad distribution in the p values at any T_c ; experimental errors coming from, e.g., some images of poor quality may be one reason, and the local fluctuation of the values themselves may be another. Their average values were, therefore, adopted to estimate ξ . It should be noted that the average p values are quite reasonable to explain the feature in the ED pattern: Not only are they greater than 0.5 but also they are closer to 0.5 than the p values for the solution-grown single crystals, being consistent with the broader feature of the streak in the ED pattern (Figure 2).

Figure 7 is the T_c dependence of ξ . For calculation of ξ using eq 4, we assumed that T_m^0 for the melt-crystallized specimens is 285 °C¹² and that $K/\Delta h_f = 180$ K by using parameters shown in ref 5. The results from the solution-grown single crystals⁵ were also plotted in this figure (below 490 K). Though there are considerable deviations from the line at 503 K (230 °C) and 523 K (250 °C), the extrapolation of the line from the solution-crystallization experiment passes through the data obtained by the melt-crystallization experiment. That is, the plot indicates that $\xi < 0$ for melt crystallization and the T_c dependence of ξ holds the linearity. Since the quality of the data, viz., that of the original images, was not so good for the specimens crystallized at 230 and at 250 °C, the deviation from the line for the results obtained at these temperatures ought to be neglected as experimental errors. On the basis of the intensity distribution of the ED pattern, it is truly reliable that, at least, $\xi < 0$ when T_c is between 230 and 250 °C.

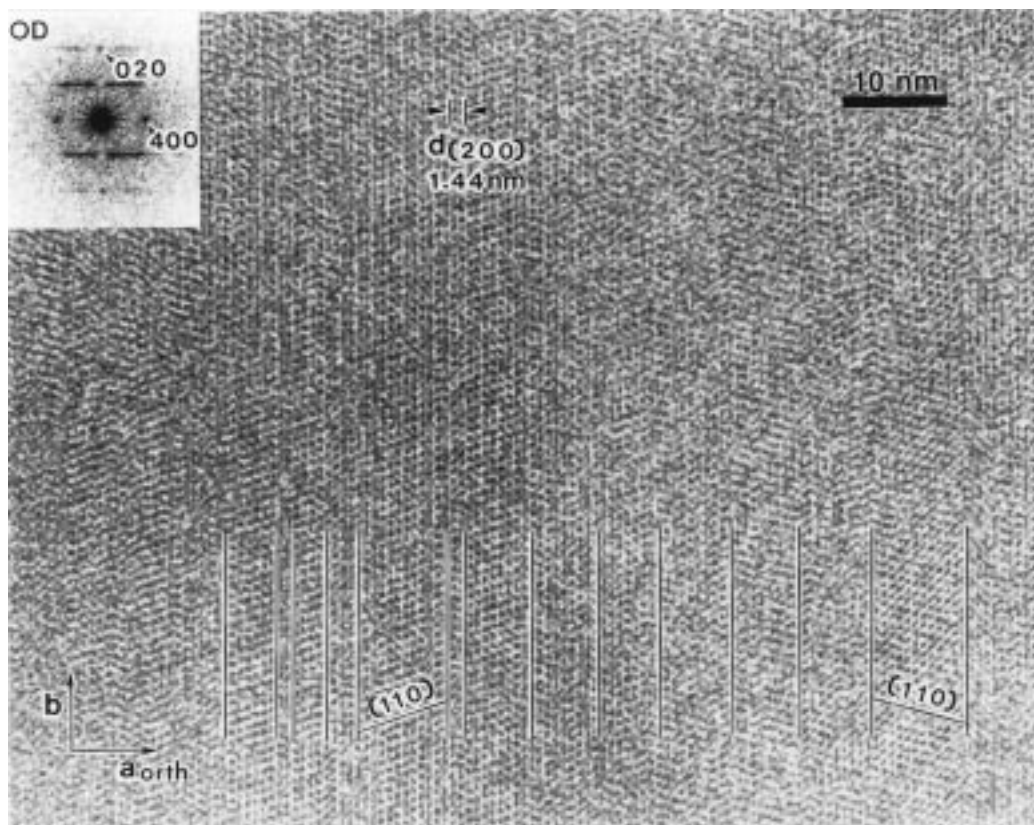


Figure 4. HREM image of the lamella of s-PS grown from the melt at 245 °C. The inset is the optical diffractogram of the original negative. Indexing the reflections in the diffractogram was carried out on the basis of the orthorhombic unit cell reported for the β'' -modification. A domain with strong (110) fringes and one with $(\bar{1}10)$ fringes are stacking alternately in the a -axis direction, as is indicated in the figure. The arrangement of molecular stems which is illustrated in Figure 3 is clearly visualized in the central part of this figure. In this image, p was estimated to be 58%.

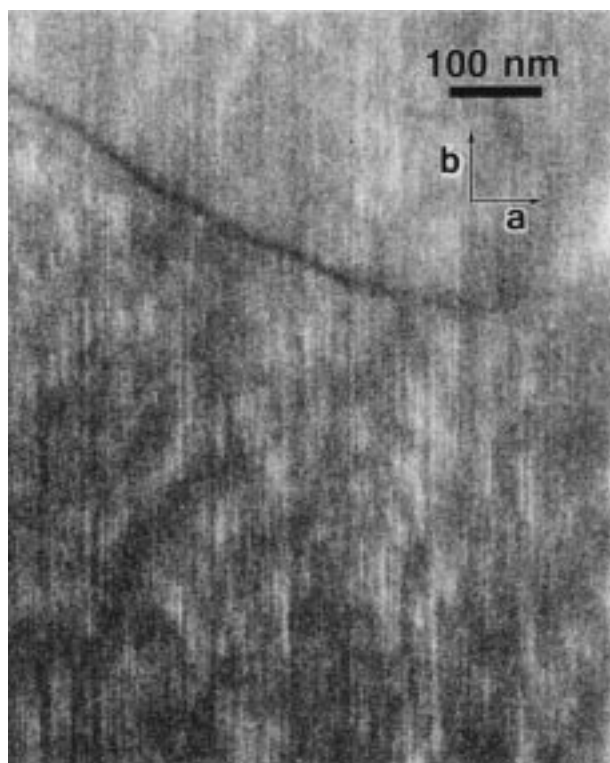


Figure 5. DF image of the lamella of s-PS grown from the melt at 240 °C.

Now, we should discuss the propriety of plotting the data obtained from two different series of experiments

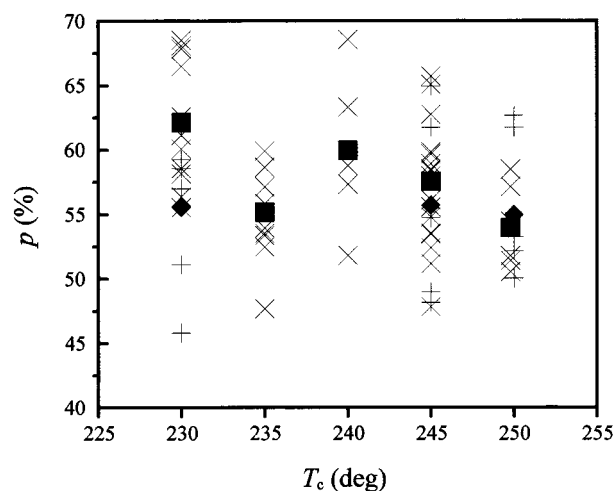


Figure 6. T_c dependence of p for the s-PS β -form: (x) measured by the HREM method, (■) average value obtained by the HREM method; (+) measured by the DF method, (◆) average value obtained by the DF method.

at the same time in Figure 7. The differences between this experiment and the previous one⁵ are the crystallization method (melt crystallization and solution one, respectively) and the molecular weight of the sample; the previous experiment was performed for the solution-grown single crystals of low-molecular-weight materials ($M_w = 7 \times 10^4$) in refs 4 and 5, and the experiment in this article uses differently prepared samples of higher molecular weight ($M_w = 1.6 \times 10^5$). In each crystal lamella, however, the energy difference, ΔE or ξ , should

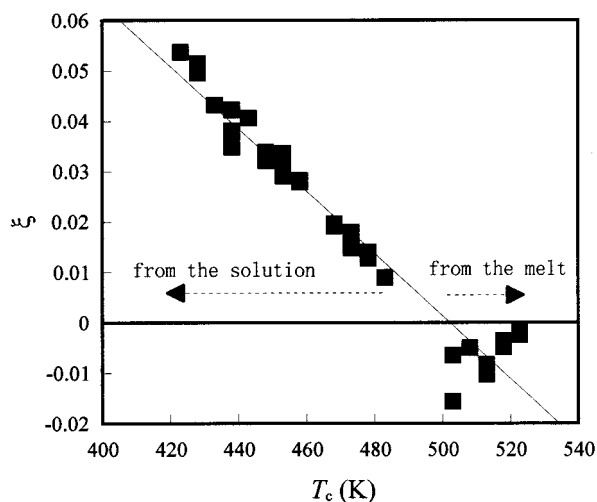


Figure 7. Dependence of ξ on crystallization temperature (T_c). The straight line was determined with the method of least squares. Regime II was assumed as in ref 5.

result only from the geometrical difference in molecular-stem arrangement between the orthorhombic and the monoclinic crystallites; other factors including the molecular weight should equally affect the growth of both types of crystallites because the crystallites in question are formed in one crystal lamella from a specific s-PS sample by a specific method. Accordingly, most of the factors except the ones that are explicitly shown in the formulation of ξ (eq 4), i.e., factors that were packed in C of eq 1, were canceled out. That is to say, the difference in the crystallization method and the molecular weight will not affect the T_c dependence of ξ .

Concluding Remarks

According to the analysis of the ED pattern from the s-PS β' -modification, the p values were greater than 0.5. This means that the succession of the motifs of a same type comprising the monoclinic layer, viz., of the "faulted" structures, is the dominant structure. This is neither the previously reported structure⁸ for the β' -modification nor the simple consequence from the Boltzmann law. Without introducing the T_c dependence of relative stability of competing two types of structures, the results presented here could not be explained. Accordingly, the idea that ΔE depends on T_c should be quite reasonable.

Furthermore, the linear T_c dependence of ξ ($=\Delta E/\Delta h_f$) which was obtained by the solution-crystallization experiment⁵ was extrapolated to higher T_c 's by carrying out the melt-crystallization experiment. This means that our theoretical treatment should be reasonable and that our view about the T_c dependence of the population of faulted structures should be supported; if the less faulted crystal is desired, the higher T_c should be selected.

On the basis of the view that is presented and is experimentally supported in this series of studies, the complicated crystallization behavior of the s-PS β -form is summarized as follows. (1) At a sufficiently low T_c (large ΔT) which is below the critical temperature (around 220–230 °C, at which $\xi = 0$),⁵ the alternation of two types of motifs (viz., orthorhombic layer) is favored. The occasional occurrence of the succession of motifs of a same type (viz., monoclinic layer) results in the stacking fault. The resulting crystal should be attributed to the β'' -modification. (2) With an increase in T_c , the relative stability of the orthorhombic layer decreases, and accordingly, the driving force to incorporate the monoclinic layer may increase. On the other hand, the chance to incorporate the monoclinic layer (viz., the high-energy structure) decreases according to the view presented in this study. As a result of compensation between these effects, the T_c dependence of p becomes very weak. (3) Above the critical temperature, the stacking fault turns to be a favorable structure. The crystal form grown in this temperature range is the β' -modification, in which a succession of motifs of a same type comprises a monoclinic domain.

Acknowledgment. The authors are indebted to Dr. T. Ogawa, Professor S. Isoda, and Professor T. Kobayashi (Laboratory of Crystal Information Analysis, Institute for Chemical Research, Kyoto University) for obtaining the HREM images using JEM-4000SFX. This work was partly supported by the Society of Fiber Science and Technology, Japan, through the Young Scientist Award (to M. Tosaka, 1998).

References and Notes

- (1) Guerra, G.; Vitagliano, V. M.; De Rosa, C.; Petraccone, V.; Corradini, P. *Macromolecules* **1990**, *23*, 1539.
- (2) Tsuji, M.; Okihara, T.; Tosaka, M.; Kawaguchi, A.; Katayama, K. *MSA Bull.* **1993**, *23*, 57.
- (3) Tosaka, M.; Hamada, N.; Tsuji, M.; Kohjiya, S.; Ogawa, T.; Isoda, S.; Kobayashi, T. *Macromolecules* **1997**, *30*, 4132.
- (4) Hamada, N.; Tosaka, M.; Tsuji, M.; Kohjiya, S.; Katayama, K. *Macromolecules* **1997**, *30*, 6888.
- (5) Tosaka, M.; Hamada, N.; Tsuji, M.; Kohjiya, S. *Macromolecules* **1997**, *30*, 6592.
- (6) Tosaka, M.; Tsuji, M.; Cartier, L.; Lotz, B.; Kohjiya, S.; Ogawa, T.; Isoda, S.; Kobayashi, T. *Polymer* **1998**, *39*, 5273.
- (7) Chatani, Y.; Shimane, Y.; Ijitsu, T.; Yukinari, T. *Polymer* **1993**, *34*, 1625.
- (8) De Rosa, C.; Rapacciuolo, M.; Guerra, G.; Petraccone, V.; Corradini, P. *Polymer* **1992**, *33*, 1423.
- (9) Hoffman, J. D.; Davis, G. T.; Lauritzen, J. I., Jr. In *Treatise on Solid State Chemistry*; Hannay, N. B., Ed.; Plenum Press: New York, 1979; Vol. 3, 7, pp 497–614.
- (10) Hoffman, J. D.; Miller, R. L. *Polymer* **1997**, *38*, 3151.
- (11) Lovinger, A. J.; Lotz, B.; Davis, D. D.; Padden, F. J., Jr. *Macromolecules* **1993**, *26*, 3494.
- (12) Arnauts, J.; Berghmans, H. *Polym. Commun.* **1990**, *31*, 343.

MA9810518